Comparison of load shifting incentives for low-energy buildings with heat pumps to attain grid flexibility benefits

Dieter Patteeuw[a,c,*], Gregor P. Henze[b], Lieve Helsen[a,c,*]

[a]*KU Leuven Energy Institute, Division Applied Mechanics and Energy Conversion, Department of Mechanical Engineering, KU Leuven, Celestijnenlaan 300 box 2420, B-3001 Leuven, Belgium*
[b]*Dept. of Civil, Environmental and Architectural Engineering, University of Colorado, Boulder, Colorado, USA*
[c]*EnergyVille, Thor Park, Waterschei, Belgium*

Abstract

This paper aims at assessing the value of load shifting and demand side flexibility for improving electric grid system operations. In particular, this study investigates to what extent residential heat pumps participating in load shifting can contribute to reducing operational costs and CO_2 emissions associated with electric power generation and how home owners with heat pump systems can be best motivated to achieve these flexibility benefits. Residential heat pumps, when intelligently orchestrated in their operation, can lower operational costs and CO_2 emissions by performing load shifting in order to reduce curtailment of electricity from renewable energy sources and improve the efficiency of dispatchable power plants. In order to study the interaction, both the electricity generation system and residences with heat pumps are modeled. In a first step, an integrated modeling approach is presented which represents the idealized case where the electrical grid operation in terms of unit commitment and dispatch is concurrently optimized with that of a large number of residential heat pumps located in homes designed to low-energy design standards. While this joint optimization approach does not lend itself for real-time implementation, it serves as an upper bound for the achievable operational cost savings. The main focus of this paper is to assess to what extent load shifting incentives are able to achieve the aforementioned savings potential. Two types of incentives are studied: direct load control and dynamic time-of-use pricing. Since both the electricity generation supply system and the residential building stock with heat pumps had been modeled for the joint optimization, the performance of both load shifting incentives can be compared by separately assessing the supply and demand side. Superior performance is noted for the direct-load control scenario, achieving 60% to 90% of the cost savings attained in the jointly optimized best-case scenario. In dynamic time-of-use pricing, poor performance in terms of reduced cost and emissions is noted when the heat pumps response is not taken into account. When the heat pumps response is taken into account, dynamic time-of-use pricing performs better. However, both dynamic time-of-use pricing schemes show inferior performance at high levels of residential heat pump penetration.

Keywords: Electricity price, direct load control, heat pump, load shifting, electricity generation, integrated assessment model

*Corresponding authors
Email addresses: `dieter.patteeuw@kuleuven.be` (Dieter Patteeuw), `lieve.helsen@kuleuven.be` (Lieve Helsen)

Nomenclature

$\mathbf{A}$	State space model matrix
$\mathbf{B}$	State space model matrix
$co_2t_{i,j}$	CO_2 emission cost
cur_j	Curtailment of RES
d_j^{HP}	Heat pump electricity demand
d_j^{IM}	Centrally-suggested demand profile
d_j^{trad}	Traditional electricity demand
$fc_{i,j}$	Fuel cost
$g_{i,j}^{PP}$	Power plant electricity generation
g_j^{RES}	RES electricity generation
nb	Number of buildings
$p_{s,j}^{AUX}$	Electricity demand auxiliary
$p_{s,j}^{HP}$	Electricity demand heat pump
$price_j^G$	Price profile from generation model
$price_j^I$	Price profile from integrated model
$q_{s,j}^{DHW}$	Domestic hot water demand
q_j^S	Solar heat gains
$q_{s,j}^S$	Internal heat gains
$rc_{i,j}$	Ramping cost
$sc_{i,j}$	Start-up cost
t_j^e	Ambient air temperature
t_j^g	Ground temperature
$t_{s,j}^{max}$	Maximum comfort temperature
$t_{s,j}^{min}$	Minimum comfort temperature
$t_{s,j}$	Temperature vector
w	Weighting factor load shaping
$z_{i,j}$	Power plant commitment status
HP	Heat pump
PP	Power plant
RES	Renewable energy sources

1. Introduction

Demand response is a form of demand-side management for altering consumers' electrical demand profiles by means of incentives such as dynamic electricity prices [1]. According to Strbac [2], demand response can reduce the need for investments in electricity generation, transmission, and distribution infrastructure, as well as mitigate negative effects associated with the large-scale introduction of generation from intermittent and variable renewable energy sources (RES). Among the multiple methods to attain demand response, as discussed by Gellings [3], this paper focusses on load shifting. In this paper, load shifting is employed to avoid electricity demand at times when power plants with lower efficiency are running and to increase demand at times when renewable energy sources are curtailed. There are various methods to attain load shifting with minimal to no impact on process quality [4], including the process of providing heating or cooling in a building context. Load shifting of heating and cooling demand can either be performed manually by the building occupants or automatically. As shown by Wang et al. [5] and Dupont [6], automatic control achieves higher participation in demand response than manual control. The smart thermostat, an enabling technology to achieve automatic control for heating and cooling demand [7], has drastically increased its market share in recent years [8]. Apart from improving energy efficiency [9], some of these internet-connected smart thermostats already perform peak shaving while maintaining thermal comfort [10].

In the literature, one can find two approaches to determining the potential benefits of load shifting, either from a grid perspective or a building owner's perspective. In order to evaluate the potential benefits of load shifting from an electric system perspective, authors typically consider direct load control [11, 12, 13, 14, 15]. In this way, applying load shifting to residential buildings with heat pumps allows numerous benefits, such as balancing short-term power fluctuations of wind turbines [11], providing reserves [12] or voltage stability [13], reducing wind energy curtailment by up to 20% [14], and reducing CO_2 emissions by up to 9% [15].

On the other hand, studies conducted from a building owner's perspective typically consider a wholesale electricity price profile and assume the actions taken under load shifting do not effect this price profile. For example, Kamgarpour et al. [16] found that for a set of 1000 residential buildings, savings of up to 14% can be attained with respect to a wholesale electricity price profile. Henze et al. [17] attained savings up to 20% by employing the passive energy storage present in an office building with respect to an on-peak and off-peak electricity tariff. Kelly et al. [18] also investigated the use of thermal energy storage to shift electricity demand to off-peak periods, but reported significant increases in energy use. In addition, Kelly et al. observed a loss of load diversity causing a peak demand during off-peak tariff periods (rebound), which is up to 50% higher than normal. This loss of load diversity phenomenon for thermostatically controlled loads is explained well by Lu and Chassin [19]. More advanced and dynamic price profiles have been suggested in different studies, e.g. Oldewurtel et al. [20] suggest a price profile based on the spot price and on the level of the traditional electricity demand. A good overview of different price based incentives for consumers is provided by Dupont et al. [21].

The motivation for the work presented in this paper revolves around the question what value grid flexibility offers. While there appears to be universal agreement that elasticity in electrical demand will be instrumental in dealing with variable and intermittent RES, little is known regarding the quantitative extent of the benefits resulting from load flexibility vis-a-vis conventional supply side options for accommodating the RES variability. This work begins this valuation of grid flexibility by investigating the optimal control of thermostatically controlled loads of electrically driven heat pumps under a set of simplifying assumptions, which are necessary to solve this approximated problem in human time. Future work will consider other flexible loads including, but not limited to, electric vehicle charging, commercial building thermal mass and HVAC systems control, and dispatchable home appliances.

In this research a unique approach is suggested and evaluated: First, both the electricity generation system and the buildings equipped with heat pumps are modeled and optimized *jointly* in order to evaluate the theoretically maximum benefits and impact of load shifting, similar to [22, 23]. Modeling both systems also allows studying different load shifting incentives. Both supply and demand systems are assumed to behave rationally and strive to minimize their observed cost. To this aim, all buildings considered feature a model predictive controller (MPC) developing optimal thermostat setpoint strategies. This could be achieved, for example, by a massive deployment of smart thermostats performing MPC. In this context, MPC is a control approach, which optimizes the control of a building's heating and/or cooling system by harnessing a simplified physical model of the building's thermal characteristics and energy systems along with predictions on occupancy and weather conditions. As shown in experiments in tertiary buildings by Široký et al. [24], MPC can reduce energy use up to 28% . Buildings with MPC can easily cope with dynamic price profiles, as shown by Oldewurtel et al. [20].

The aim of this paper is twofold. First, it is of interest how much operational costs and CO_2 emissions of the electric system can be reduced by a widespread application of load shifting for low-energy residential buildings equipped with electric heat pumps. Hence, this paper does not consider the potential of load shifting in alleviating grid congestion, providing spinning reserves, offering frequency regulation, or providing voltage stability. Instead, this paper aims at assessing, in a deterministic manner, how much fossil fuel use and RES curtailment can be avoided at the electric system level. The main focus of the paper is to compare two common approaches to attain the desired benefits through load shifting with a practical implementation in mind: direct-load control and time-of-use pricing. These incentives are compared by determining to what extent the reductions in operational costs and CO_2 emissions, as enabled by load shifting, are attained. The results of the first part involving the joint optimization of energy supply and demand system serve as a reference benchmark for this comparison.

In this study, the presented models are built on many simplifying assumptions. All models employ perfect predictions and assume the absence of model mismatch. All buildings possess ideal model predictive controllers and have an identical building structure. The heat pumps have a predetermined, fixed COP for each optimization horizon and can modulate perfectly. There are no constraints and losses of the transmission and distribution grids. Also, there is no import or export of electricity. Finally, there is perfect competition among all power plants and buildings.

This paper will show that, even under these strong assumptions and simplified deterministic assessment, the performance of the studied load shifting incentives already significantly deviates from the load shifting performance of the jointly optimized best-case scenario. Additionally, it is shown that this performance is very sensitive to the share of RES and the number of participating buildings.

The boundary conditions in this study are inspired by the Belgian context, with an electricity generation system dominated by nuclear power plants, gas-fired power plants, and renewable energy sources (RES). The buildings considered are all detached, heating-dominated low-energy buildings. As shown by Patteeuw et al. [23], low-energy buildings are the best candidates for a widespread heat pump implementation in Belgium. Section 2 describes the different models and scenarios employed in this paper. The Results Section (Section 3) illustrates the output of the different models (Section 3.1) used to evaluate the load shifting potential (Section 3.2) and the performance of load shifting incentives (Section 3.3). The difference between the performance of these load shifting incentives is explained in Section 3.4 while results for mixtures of these incentives are shown in Section 3.5. Finally, a discussion is given in Section 4 in order to arrive at the conclusions in Section 5.

2. Methodology

This section consists of two parts. Section 2.1 elaborates on the different models used, and the case study for assessing the load shifting incentives. Section 2.2 illustrates the different scenarios considered for applying these incentives.

2.1. Models and parameters

All models in this article are examined as deterministic optimal control problems as listed in Table 1. In the first model (Gen), the electricity generation system minimizes its total operational cost via a unit commitment and economic dispatch problem with profiles for electricity demand and electricity generation by RES. From a building owners' perspective (B20 and B2), the heat pumps in the buildings

Table 1: Overview of the abbreviation (Abbr.) and description of the models in this study.

Abbr.	Description
Gen	Electricity generation system model
B20	Large building stock model, optimal control problem of 20 buildings.
B2	Aggregated building stock model based on B20.
Int20	Integrated model performing a co-optimization of B20 and Gen.
Int2	Integrated model performing a co-optimization of B2 and Gen.

are controlled by MPC that minimizes individual electricity cost while maintaining thermal comfort. In the integrated models, the two optimal control problems are combined into one optimal control problem (Int20 or Int2) that jointly minimizes the total cost for generating electricity for both the traditional electricity demand and the total electricity demand, including that stemming from low-energy buildings with heat pumps whose temperature setpoints can be optimized. These models are mixed integer linear programs (MILP) with an optimality gap of 0.1%, implemented in GAMS 24.4 and MATLAB 2011b, using the MATLAB–GAMS coupling as described by Ferris [25] with CPLEX 12.6 as solver. All presented results are from a full year simulation for which the electricity demand and weather conditions are based on Belgium in 2013.

Electricity generation system. The electricity generation system is modeled as a unit commitment and economic dispatch problem [26]. For every time step j, the commitment status (binary variable $z_{i,j}$) and the hourly output of each power plant with index i ($g_{i,j}$) are determined along with the curtailment of renewable energy sources (cur_j) in order to minimize the total operational cost of meeting the electricity demand:

$$\min \sum_{i,j} fc_{i,j} + co_2t_{i,j} + sc_{i,j} + rc_{i,j} \tag{1}$$

subject to

$$\forall j : d_j^{trad} + nb \cdot d_j^{HP} = cur_j \cdot g_j^{RES} + \sum_i g_{i,j}^{PP} \tag{2}$$

$$\forall j : 0 \leq cur_j \leq 1 \tag{3}$$

$$\forall i,j : f(g_{i,j}^{PP}, z_{i,j}) = 0. \tag{4}$$

The total cost consists of fuel cost ($fc_{i,j}$), CO_2 emission costs ($co_2t_{i,j}$), and costs related to starting ($sc_{i,j}$) and ramping ($rc_{i,j}$) of power plants. Electricity generation from renewable energy sources (g_j^{RES}) is assumed to have an operational cost of zero. As described in Appendix A or by Patteeuw et al. [27], the constraints ($f(g_j^{PP}, z_{i,j})$) include minimum and maximum operating points, ramping rates, minimum up and down times and start-up costs. The electricity demand consists of two parts. The first is the traditional national-scale electricity demand, assumed to remain a fixed profile ($d_{\mathrm{j}}^{\mathrm{trad}}$). The second part is the electricity demand of the heat pumps ($d_{\mathrm{j}}^{\mathrm{HP}}$). Given the load diversity due to the difference in user behavior, as discussed in the text below, the electricity demand of the heat pumps is scaled linearly with a factor nb and hence represents the demand of a large portfolio of buildings. In order to study the magnitude sensitivity, the number of buildings is varied in multiple steps between $50,000$ and $500,000$. Hence, on a yearly basis, the heat pumps of the buildings respectively add an electricity demand between 0.4 and 4 TWh to the traditional electricity demand of 85.6 TWh [28], i.e. at most roughly 5%.

The technical parameters and fuel costs for the power plants are taken from Bruninx et al. [29] and summarized in Table 2. These technical parameters and costs are inspired by

Table 2: Parameters for the electricity generation system per fuel type [29, 30, 28, 31]

Type	Total cap. (MW)	Nr. of units (-)	Nominal cost ($\frac{EUR}{MWh_e}$)
Nuclear	5925	8	6
Coal	760	3	30
Gas	7018	47	60
Oil	215	13	83

the Belgian power system. However, in order to cope with the large production by RES, the technical parameters for the nuclear power plants are taken from more flexible nuclear power plants than currently present in Belgium. Hence, the generation system is inspired by, but not completely representative for Belgium. Additionally, as mentioned in the beginning of the Methodology section, losses or capacity limits due to the electricity grid are neglected.

The profile for the traditional electricity demand (d_j^{trad}) consists of the Belgian electricity demand, from which the electricity generation by combined heat and power, run-off river, and pumped hydro are subtracted. The profiles for these demand and generation types are assumed to be constant and are taken from Elia [30] for Belgium for the year 2013. Electricity generation from PV, onshore wind and offshore wind is lumped together in g_j^{RES} with a share based on the year 2013 in Belgium [30]: 3%, 2.2% and 2.7%, respectively. The generation profiles of these RES are also for Belgium in the year 2013 [30]. In order to study the sensitivity of the results towards the share of electricity generation from RES, the generation profile is scaled up in order to represent 15%, 20%, 30% and 40% of the yearly electricity demand, depending on the case. According to Devogelaer et al. [32], these are feasible shares for Belgium.

Residences with heat pumps. Regarding the residences with heat pumps, the individual cost minimization is a linear optimal control problem, towards minimizing the total electricity demand ($\sum_j d_j^{HP}$) of multiple buildings, denoted by the index s:

$$\min \quad \sum_j d_j^{HP} = \sum_s \left(p_{s,j}^{HP} + p_{s,j}^{AUX}\right) \tag{5}$$

subject to

$$\begin{aligned} \forall s,j : t_{s,j+1} &= \mathbf{A} \cdot t_{s,j} \\ &+ \mathbf{B} \cdot [p_{s,j}^{HP}, p_{s,j}^{AUX}, t_j^e, t_j^g, q_j^S, q_{s,j}^I, q_{s,j}^{DHW}] \end{aligned} \tag{6}$$

$$\forall s,j : t_{s,j}^{min} \leq t_{s,j} \leq t_{s,j}^{max}. \tag{7}$$

The demand for space heating and domestic hot water (DHW) is either provided by an air-coupled heat pump ($p_{s,j}^{HP}$) or by an auxiliary electrical resistance heater ($p_{s,j}^{AUX}$). The building structure is a reduced-order model based on Reynders et al. [33] and illustrated in Figure 1. The combination of reduced-order models of heating system and building model shows a RMSE of 5 % per building with respect to a detailed emulator model [34]. The vector $t_{s,j}$ denotes the temperatures of this building structure, along with the average temperature of the DHW storage tank. These temperatures are determined by a state-space model (matrices $\mathbf{A}$ and $\mathbf{B}$) and subject to disturbances. These disturbances consist of the ambient air temperature (t_j^e), ground temperature (t_j^g), solar heat gains (q_j^S), internal heat gains ($q_{s,j}^I$) and DHW demand ($q_{s,j}^{DHW}$). The indoor air temperatures as well as the temperature of the storage tank for DHW need to stay within the lower ($t_{s,j}^{min}$) and upper ($t_{s,j}^{max}$) bound in order to maintain thermal comfort. An overview of the model equations is given in Appendix A while a detailed description and verification of the model equations is given by Patteeuw and Helsen [34].

In order to keep the problem size for the best case integrated model (Int20) manageable for the MILP solver, the number of buildings, with index s was chosen to be 20. Each of the 20

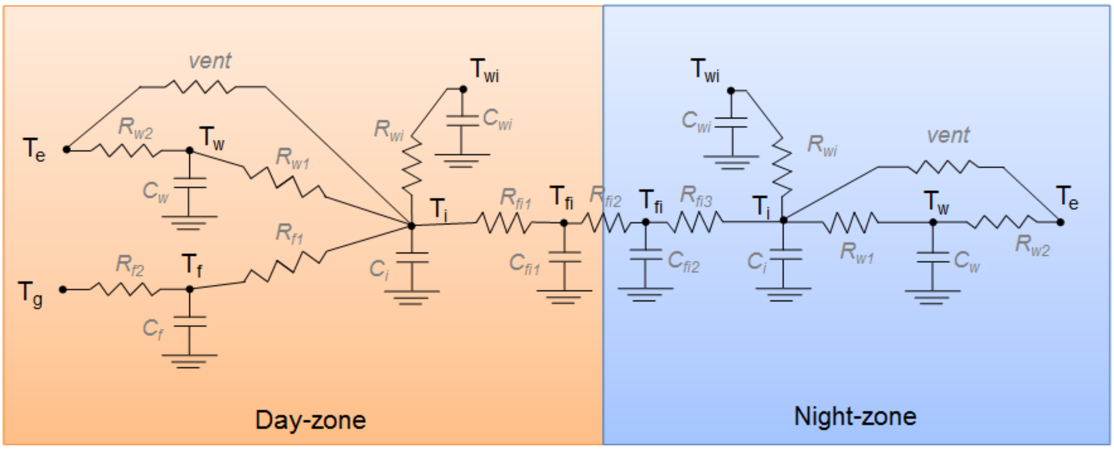

Figure 1: The structure of the reduced order building model as developed by Reynders et al. [33]. The day zone consists of 5 states: the temperatures of the indoor air (T_i), internal walls (T_{wi}), external walls (T_w), ground floor (T_f) and floor connecting the day zone and night zone (T_{fi}). The night zone also has a state for this connection, along with a temperature for indoor air, internal walls and a lumped state for external walls and roof (T_w). The parameters for the different R and C values can be derived based on Protopapadaki et al. [35]. The ambient air temperature (T_e) and ground temperature (T_g) are boundary conditions to the model.

buildings has a different user behavior, based on Baetens and Saelens [36], but an identical building structure. This results in a diversity factor of 75 %, similar to the active occupancy of Richardson et al. [37]. Hence, the buildings are assumed to be represented by an average building, as the load shifting potential for thoroughly insulated buildings is very similar [23]. This average building is split up in two thermal zones as proposed by Reynders et al. [33] (see Figure 1). The first zone, named “day zone”, consists of the ground floor and includes the rooms where the occupants are active by day. The other rooms, consisting mainly of bedrooms, make up the second zone named “night zone”. Based on the TABULA [38] project in which representative buildings for the Belgian building stock were investigated, the day and night zone have a floor area of 132 m^2 and 138 m^2 respectively. Furthermore, this study focuses on low-energy buildings. According to the economic optimum for Belgium [39], these buildings have an average U-value of 0.3 W/m^2K and a ventilation rate of 0.4 air changes per hour (ACH).

Each building is equipped with floor heating and a hot water storage tank for domestic hot water, which are both heated by an air coupled heat pump. The heat pump is sized to meet 80% of the peak heat demand while the rest of the peak demand is covered by an auxiliary electric resistance heater. The coefficient of performance (COP) of the heat pump is predetermined according to Bettgenhäuser et al. [40] and assumed constant throughout each optimization horizon of a week. The constant COP assumption in optimal control problems has been studied by Verhelst et al. [41] and Patteeuw and Helsen [34]. Finally, weather data is based on measurements in Uccle (Brussels, Belgium).

Integrated model. In the integrated model, the two above mentioned optimal control problems are merged into one optimal control problem. The buildings no longer minimize their own electricity use and Eq. (5) becomes a constraint instead of an optimization criterion. Hence, the objective function is the total operational cost minimization of meeting the electricity demand, with the added freedom of shaping the heat pumps' electricity demand:

$$\min \sum_{i,j} fc_{i,j} + co_2t_{i,j} + sc_{i,j} + rc_{i,j} \tag{8}$$

subject to

$$\forall j : d_j^{trad} + nb \cdot d_j^{HP} = cur_j \cdot g_j^{RES} + \sum_i g_{i,j}^{PP} \tag{9}$$

$$\forall j : 0 \leq cur_j \leq 1 \tag{10}$$

$$\forall i, j : f(g_{i,j}^{PP}, z_{i,j}) = 0 \tag{11}$$

$$\forall j : d_j^{HP} = \sum_s \left(p_{s,j}^{HP} + p_{s,j}^{AUX}\right) \tag{12}$$

$$\begin{aligned} \forall s, j : t_{s,j+1} &= \mathbf{A} \cdot t_{s,j} \\ &+ \mathbf{B} \cdot [p_{s,j}^{HP}, p_{s,j}^{AUX}, t_j^e, t_j^g, q_j^S, q_{s,j}^I, q_{s,j}^{DHW}] \end{aligned} \tag{13}$$

$$\forall s, j : t_{s,j}^{min} \leq t_{s,j} \leq t_{s,j}^{max}. \tag{14}$$

This electricity demand can be shaped as long as the indoor operative temperatures and hot water tank temperature stay between comfort bounds. The merit of this modeling approach, for which the equations are given in Appendix A or in [27], is the ability to fully capture the operational benefits of load shifting for the electricity generation system, as shown in [42].

In the ideal case, this integrated model has available all details of buildings participating in load shifting (Int20)[1]. In practice however, the number of participating buildings could go up to thousands, making an integrated optimization infeasibly large. Thus, an aggregation of this large building set is necessary. Assuming the presented average building to be representative for a wider set of buildings, an aggregation with respect to building parameters is not needed. However, the 20 buildings are considered to have different occupant behavior. An aggregation methodology [34] is employed to aggregate these buildings into two representative buildings used in the integrated model Int2 (see Table 1). The aggregation methodology consists of two steps as demonstrated in Figure 2. First, a preprocessing step is needed to determine the lowest possible temperature profiles which still provide thermal comfort (blue lines in Figure 2a and Figure 2b). This is done by performing the minimization towards electricity demand, as given by Eq. (5) to Eq. (7), to determine the lowest possible temperatures for the day zone, night zone and storage tank for DHW, one for each building. In a second step, these temperature profiles are averaged over all buildings considered (black line in Figure 2c). These averaged temperature profiles serve as lower bounds ($T_{s,j}^{min}$) for the aggregated building stock of the integrated model (Int2). In this model, only two buildings remain, with the "average" building structure but with two different sizes of the DHW storage tank.

2.2. Incentive scenarios

Given the modeling framework discussed in Section 2.1, it is possible to study different incentive mechanisms for realizing the possible operational benefits of load shifting. Figure 3 gives an overview of the different incentive scenarios.

First, in the Reference scenario, no load shifting is performed. In this scenario, the controls of the heat pumps of the 20 buildings (B20) completely ignore the electricity generation system and focus on minimizing their own electricity use. Hence, in this scenario the buildings face a flat electricity price. This results in the following optimization criterion for the optimal control problem of the MPC:

$$\min \sum_j d_j^{HP}. \tag{15}$$

[1] In some cases, the integrated optimization with 20 buildings (Int20) was not able to attain a solution. For the other cases, the results were very close to the integrated model with the aggregated buildings (Int2), more precisely within the optimality gap of 0.1%. Hence, in the failed cases of Int20, the result from Int2 serves as result for Int20.

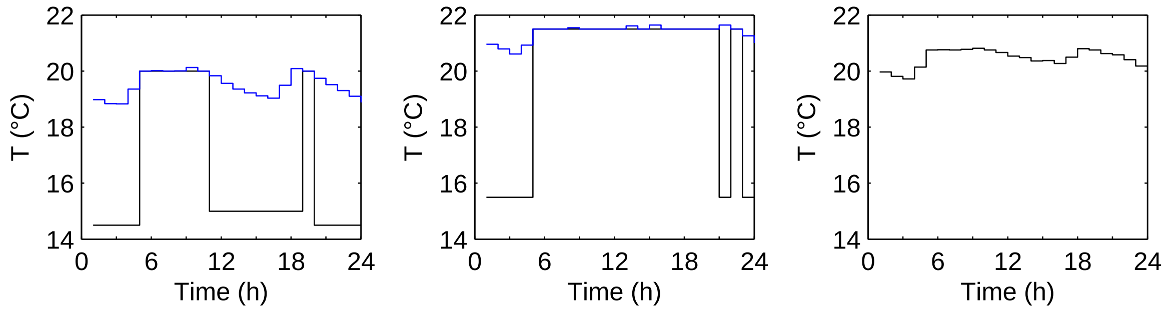

(a) Building 1 (b) Building 2 (c) Aggregated

Figure 2: Example of user behavior aggregation for 2 buildings, based on [34]. Black lines denote a lower set point for the operative temperature in the day zone. Blue lines denote the actual temperature profiles.

From this, the electricity generation system (Gen) needs to deliver this resulting heat pump electricity demand plus the traditional electricity demand.

In the Best Case scenario, the electricity generation system and all participating buildings simultaneously optimize their control by means of an integrated model (Int20). In this model, the building structure and domestic hot water tanks are occasionally preheated when this reduces the total cost for the electricity generation system. Simultaneously, the power plants are optimally dispatched in order to meet the resulting electricity demand. This Best Case scenario serves as upper bound of the operational cost savings attainable by applying load shifting.

A first time-of-use pricing scenario is the Price G scenario. In this scenario, the electricity generation system makes an estimate of the total electricity demand of the following day, including the electricity demand of the heat pumps, which minimize their own consumption. This estimate is assumed to be perfect in this paper. However, the heat pump controllers receive the resulting price profile, $price_j^G$, and alter the electricity demand accordingly by applying the following optimization criterion:

$$\min \sum_j price_j^G \cdot d_j^{HP}. \tag{16}$$

In real-time, the electricity generation faces the traditional electricity demand plus the altered building electricity demand. This scenario hence represents a unilateral price communication from the electric power system to the buildings with heat pumps.

In contrast to this, the Price I scenario represents the situation where the electricity generation system makes an estimate of the flexibility of the buildings with heat pumps. In the estimate for the following day, the aggregated representation of the buildings with heat pumps (B2) is co-optimized with the dispatch of the electricity generation system. The resulting price profile from this integrated model, $price_j^I$, is then communicated to the controllers of the heat pumps, resulting in the following optimization criterion

$$\min \sum_j price_j^I \cdot d_j^{HP}. \tag{17}$$

Also in this scenario, the impact of the measure on the electricity generation system is determined.

Finally, the Load Shaping scenario is identical to the Price I scenario except that, instead of communicating the resulting price profile, the resulting demand profile from the integrated model (d_j^{IM}) is communicated to the buildings. This demand profile, similarly to the work of Corbin and Henze [43, 44], acts

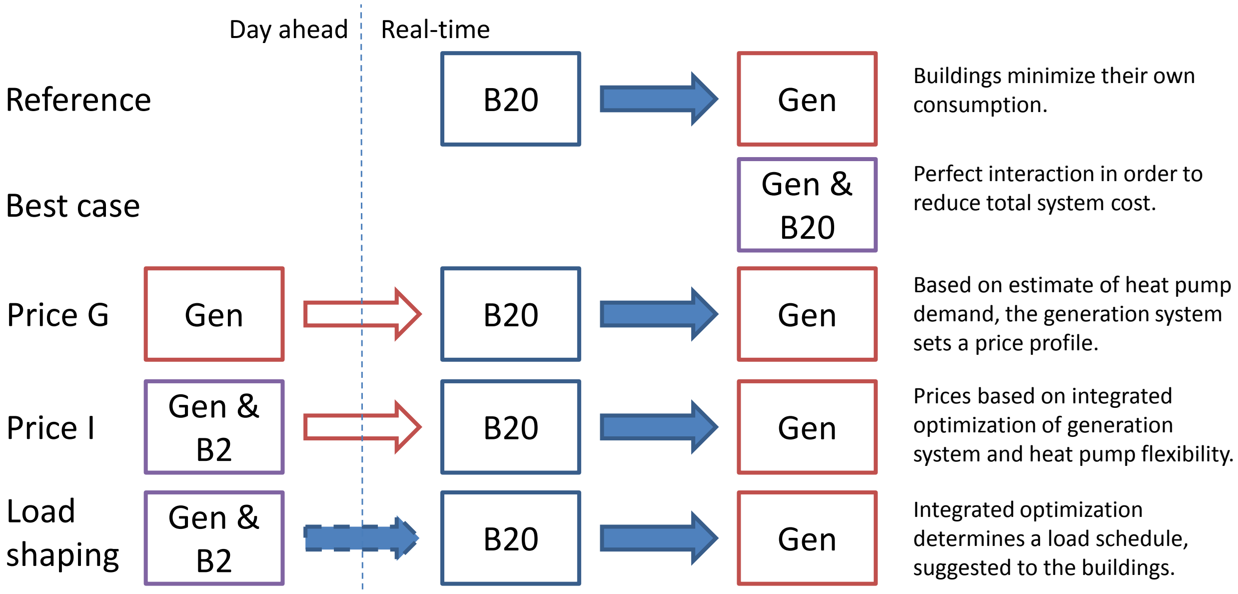

Figure 3: An overview of the studied scenario's. The red non-filled arrows denote the communication of a price profile. The blue filled arrows denote the communication of the electricity demand profile of the buildings equipped with a heat pump. In the load shaping scenario, the dashed blue arrow denotes the suggestion of an electricity demand profile. The color of the boxes denotes the model type. The red box denotes the electricity generation system model, the blue box the building stock model and the purple box the integrated model of both.

as a centrally-suggested demand curve for the buildings with heat pumps. The resulting optimization criterion for the optimal control problem of the heat pump controllers is:

$$\min w \cdot |d_j^{HP} - d_j^{IM}| + (1-w) \cdot \sum_j d_j^{HP} \quad (18)$$

in which d_j^{IM} represents the centrally-suggested demand profile from the integrated model. Hence, the heat pump controllers make a trade-off between the deviation with respect to the centrally-suggested demand profile ($|d_j^{HP} - d_j^{IM}|$) and minimizing electricity use ($\sum_j d_j^{HP}$) by means of the weighting factor w, taken to be 0.5 in this study.

3. Results

The Results Section consists of five parts. In the first part, Section 3.1, the output of the different models, presented in Table 1, is illustrated. In Section 3.2, the potential of load shifting is investigated for the studied boundary conditions. The results for the different load shifting implementation scenarios are shown in Section 3.3 and the resulting metrics in Section 3.4. Finally, the different cost functions for the buildings, Eq. (15) to (18), are combined in Section 3.5.

3.1. Illustration of model output

Figure 4 shows the results for two days in the case where 30% of the yearly electricity demand is generated from RES and 250,000 buildings are equipped with heat pumps. The power plants need to generate the sum of the residual traditional electricity demand, Figure 4a, and the electricity demand of the heat pumps, Figure 4c. Note that, in some scenarios, both the heat pump and auxiliary heater are activated simultaneously, causing a high electricity demand of $10kW_e$ per building. Figure 4b shows how the day zone temperatures, averaged over the buildings, are manipulated to achieve these electricity demands. In the

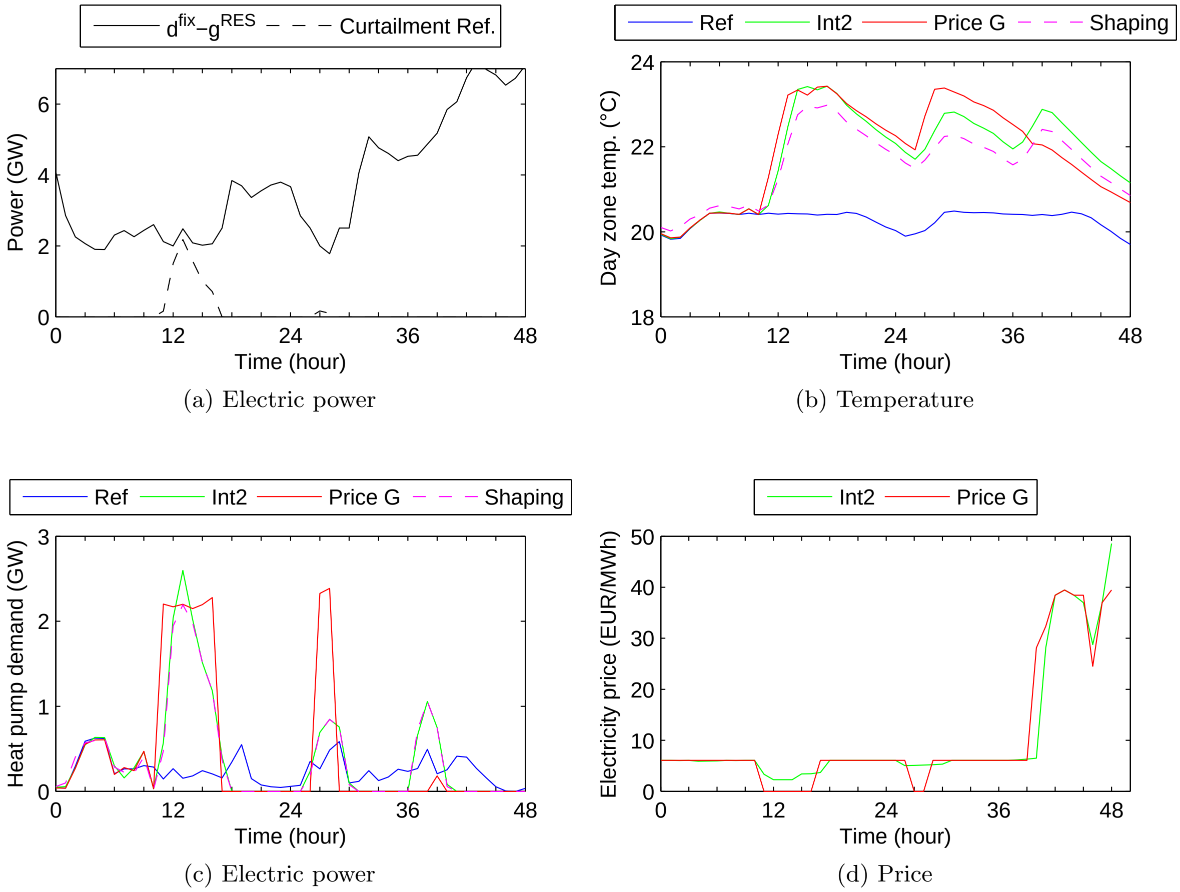

(a) Electric power

(b) Temperature

(c) Electric power

(d) Price

Figure 4: The power plants must deliver the sum of the traditional residual demand (Figure 4a) and the heat pumps demand (Figure 4c). The curtailment at hours 11 to 16 and hours 27 to 28, in some cases communicated through a price profile (Figure 4d), forms an incentive to preheat the buildings (Figure 4b).

Reference scenario (blue lines in Figure 4), the indoor air temperatures are kept close to the lower comfort bounds, resulting in an electricity demand that doesn't strongly fluctuate. In this scenario, the buildings miss the opportunity of using the excess electricity generation by RES that gets curtailed in hours 11 to 16 and hours 27 to 28. In the Best Case scenario (green lines in Figure 4) advantage of this abundant electricity generation by RES is taken by drastically increasing heat pump electricity demand (d_j^{HP}) in those hours. As a result, no electricity generation by RES is curtailed, as the buildings have perfect knowledge of the magnitude of the curtailment. This avoiding of curtailment causes the nuclear power plants to set the price (green line in Figure 4d) and, hence, no zero electricity price is observed.

This is not the case for the Price G scenario (red lines in Figure 4). In this scenario, the buildings face a zero electricity price at times of curtailment, see Figure 4d. This causes the so-called avalanche effect [45] to occur, meaning that the buildings drastically increase their electricity demand as they observe electricity to be completely for free at that time. However, this leads to an overshoot in demand, which will cause the electricity price to go up again in hours 11, 15, 16, 27 and 28. Clearly, this will increase the electricity generation cost far more than expected. The Load Shaping scenario (pink dashed lines in Figure 4) does not cause this overshoot in demand, as it receives information on how much to increase electricity use in these time periods. As can be seen in the figure, the electricity demand profile in the Load Shaping scenario is very close to that of the Best Case scenario.

3.2. Potential of load shifting

In this section, the savings in operational cost and CO_2 emission of the Best Case scenario for load shifting are shown. This will serve as an upper bound to the possible savings of the different load shifting implementation scenarios in Section 3.3. Throughout this paper, the results are given for a variation of two important parameters: The number of buildings equipped with heat pumps and the share of electricity generated by RES over a year. Table 3 gives an overview of the total yearly operational cost and CO_2 emissions. Note that the mentioned number of buildings switch from fossil fuel fired heat production to heat pumps. A higher number of buildings making this switch, causes a higher electricity demand and thus higher operational costs and CO_2 emissions for the electricity generation system[2].

As can be seen in Table 3, performing load shifting causes operational costs and CO_2 emissions to decrease. The trend is however not linear, as can be seen in the savings per participant. This is discussed further by Arteconi et al. [46]. A number of buildings higher than 500,000 is not studied as the peak in total demand approaches the maximum installed capacity of the assumed electricity generation system. A number of buildings lower than 50,000 is also not studied as for these small numbers, the operational cost savings approach the optimality gap of 0.1% used in this study.

Another important parameter is the share of electricity generated by RES over a year. As can be seen in Table 3, a higher share of RES causes the potential operational cost savings of load shifting to increase. For example, an increase in RES share from 8 to 40%, causes the potential operational cost savings to rise from 12 million EUR to 28 million EUR.

3.3. Comparison of incentives scenarios

The savings presented in Section 3.2 could be hard to attain in practice as the Best Case scenario is not feasible for a large set of buildings. Instead, a set of alternative scenarios for attaining these savings were introduced in Section 2.2. The performance of these different scenarios in striving towards the operational cost savings of the Best Case scenario is shown with respect to the RES share in Figure 5a for 250,000 buildings with heat pumps. In this figure, 100% represents the Best Case scenario, while 0% represents the Reference scenario. Most notable is the poor performance of the Price G scenario. Up to a RES share of 20%, this implementation causes the total operational cost to be even higher than the Reference scenario. This is because the buildings greedily overreact to price incentives and induce extra operational costs for the electricity generation system. Only when the RES share is high enough, does the Price G scenario start showing operational costs reductions with respect to the Reference scenario. However, this increase in savings for a higher RES share is a general trend in all scenarios.

The price signal from the integrated model, scenario Price I, partly avoids the overreaction as it has information on both electricity generation system and buildings. In a sense, it represents the price signal after a long iteration of price and demand between electricity generation system and buildings. However, the Price I scenario is still outperformed by about 20%

[2] When considering the entire system from a primary energy perspective, buildings and electricity generation system, the switch to heat pumps causes total operational costs and CO_2 emissions to lower, see Patteeuw et al. [23]. This paper only discusses the effects for the electricity generation system.

Table 3: The difference between the Reference and Best Case yields the upper limit for savings by applying load shifting. Both the relative savings and the savings per participant (part.) are shown.

RES share (%)			30			8	15	20	30	40
No. of buildings (x1000)	50	100	250	375	500			250		
Reference: cost (10^6 EUR)	670	682	723	760	799	1276	1048	916	723	595
Reference: CO_2 (10^6 ton)	4.68	4.81	5.21	5.57	5.92	10.98	8.72	7.31	5.21	3.95
Best case: cost (10^6 EUR)	663	670	697	724	755	1264	1032	896	697	567
Best case: CO_2 (10^6 ton)	4.61	4.69	4.97	5.24	5.52	10.94	8.64	7.16	4.97	3.69
Cost saving (%)	1.0	1.7	3.6	4.7	5.5	0.9	1.5	2.2	3.6	4.7
CO_2 reduction (%)	1.5	2.5	4.6	5.9	6.7	0.4	0.9	2.1	4.6	6.6
Cost saving (EUR/part.)	140	120	104	96	88	48	104	80	104	112
CO_2 reduction (ton/part.)	1.4	1.2	0.96	0.88	0.80	0.16	0.32	0.64	0.96	1.04

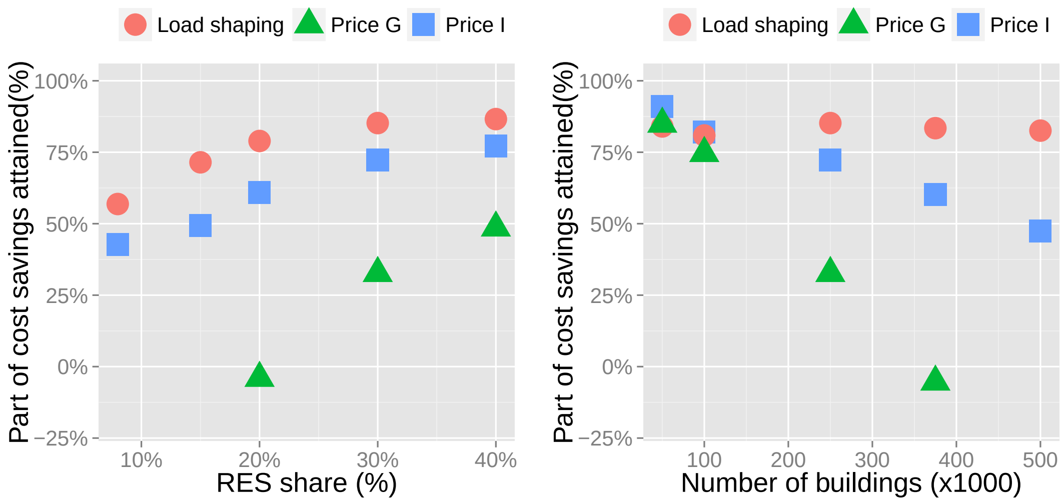

(a) For 250,000 buildings

(b) For a 30 % RES share

Figure 5: Scenario comparison for operational cost savings relative to the Best Case scenario of load shifting. In Figure 5a the share of RES is varied while 250,000 buildings are considered. In Figure 5b the number of participating buildings is varied while the RES share remains at 30%.

Table 4: The difference in operational cost savings between the different incentive scenarios can be explained by the difference in curtailment of electricity generation by RES (Curt.), the average part load of all operating power plants throughout the year (%), the difference in fuel and CO_2 cost (Fuel+CO_2) and the difference in costs related to starting up and ramping of power plants (Start-up + ramping).

Scenario	8% RES				40% RES			
	Curt. (TWh)	Part load (%)	Fuel + CO_2 (cost in 10^6 EUR)	Start-up + ramping (cost in 10^6 EUR)	Curt. (TWh)	Part load (%)	Fuel + CO_2 (cost in 10^6 EUR)	Start-up + ramping (cost in 10^6 EUR)
Reference	0	95.8	1252	24	2.27	88.3	562	33
Best Case	0	97.8	1244	20	1.12	88.8	538	30
Price I	0	96.0	1249	22	1.80	88.2	544	30
Load Shaping	0	97.1	1249	20	1.64	87.8	542	30

by the Load Shaping scenario, although the difference decreases for a higher RES share.

The difference between Price I and Load Shaping scenarios can be explained using Table 4. For a low RES share (8%), there is no curtailment in the electricity generation system and the operational cost savings by load shifting (Best Case) are dominated by improving the efficiency of the power plants (Fuel and CO_2 cost) and avoiding start-up and ramping costs. The efficiency of the power plants is improved by running these power plants closer to their full load capacity (see Part load in Table 4). These savings can be subtle to attain, as a slight increase in demand above the maximum generation capacity of the last power plant can trigger an extra power plant to be activated. Since in the Load Shaping scenario an exact indication of what the ideal electricity demand profile looks like is given, these subtleties are better retained. A price profile can give an indication of when electricity demand should be increased or decreased, but not *how much* this increase or decrease should be.

On the other hand, for a high RES share (40%), the savings are dominated by reducing RES curtailment in order to decrease operational costs. Both Price I and Load Shaping scenarios are successful in decreasing RES curtailment. In the former, the buildings see a very low electricity price and act accordingly. In the latter, the buildings receive information on how much the demand should be increased when curtailment occurs. However, the Load Shaping scenario is better as it communicates *how much* the demand should be increased in order to exactly absorb all curtailment. This information is not present in a price profile.

The number of buildings having a heat pump installed, also has an impact on the performance of the incentive scenarios as shown in Figure 5b. In this figure, the share of RES in the yearly electricity generation is fixed to 30%. First of all, the Price G scenario performs very poorly as more people install a heat pump that participates in load shifting. In the case of 500,000 buildings, the demand overshoot in the coldest week is so high that the maximum cumulative capacity of the production park is exceeded. With respect to the Price I scenario, when a relatively low number of buildings is involved, this scenario performs the best. However, as more buildings are involved, these all respond to the same price profile, and cause demand overshoots. In this case, the buildings start influencing the price itself, and become price influencers instead of price takers. In the case of 500,000 buildings with heat pumps, the performance is so abysmal that only about half of the potential savings are attained. In contrast to this, the Load Shaping scenario is far more robust to the number of buildings: No matter what this number of buildings is, the Load Shaping scenario attains about 80% of the possible savings.

3.4. Comparison on metrics

Similar to the work of Corbin [47], Table 5 presents different metrics to evaluate the improvement of the different incentive scenarios with respect to the Reference scenario. In contrast to the work of Corbin, the full electricity generation system is modeled, which allows a direct interpretation of the residual demand curve. This is the total demand from which the electricity generation from RES is subtracted ($d_j^{trad} + nb \cdot d_j^{HP} - cur_j \cdot g_j^{RES}$). In all load shifting scenarios, the electricity use of the heat pumps rises by between 13% to 20%. This is due to the high share of electricity generated by RES and nuclear power plants, which causes a lot of curtailment to occur in the Reference scenario. In the model, curtailment is deemed as for free and drastic increases in electricity use occur during these hours. This reduces electricity use after the time periods when curtailment occurred. Additionally, for the Best Case, an arbitrary choice between heat pump and auxiliary heater occurs at times of curtailment, since during these times electricity is observed as for free. The Load Shaping scenario, as shown in Eq. (18), partly minimizes own electricity use, and will mostly choose for the heat pump during times of curtailment. For the Price G scenario, the zero electricity price at curtailment causes a drastic increase in electricity use. The Price I scenario rarely observes this zero electricity price, as illustrated in Figure 4d, and hence increases electricity use far less.

The peak demand shows interesting differences between the different scenarios. During peak moments, expensive generation plants are running and the Best Case scenario will try to reduce electricity use during these hours as much as possible. The Price I and Load Shaping scenarios are able to partially imitate this behavior. However, for the Price G scenario the situation becomes worse than the Reference scenario, as an overreaction to high prices in some hours causes an even higher peak in the hours before.

Table 6: Hybrid incentive scenarios in which the optimization criteria are a mixture of minimizing energy use (Energy), minimizing cost with respect to a price profile from the generation (Price G) or the integrated model (Price I) and deviation towards a load profile (Load). The presented attained percentage of operational cost savings is for the case of a 30% RES share and 250,000 buildings with heat pump.

Name	% savings
Energy+Price G	38
Energy+Price I	41
Price I+Load	90
Energy+Price I+Load	93

The mean ramping, calculated as the mean of the absolute value of the ramping from hour to hour, shows significant differences between the scenarios. The Best Case scenario is able to significantly decrease the hour to hour variations in residual demand. The Price I and Load Shaping scenario approximate this behavior while the Price G scenario again shows worse behavior than the Reference case. This is mainly due to the drastic ramping of the heat pump electricity demand right before and after hours of curtailment, as shown in Figure 4c.

3.5. Hybrid incentive scenarios

Multiple combinations of the above mentioned scenarios are possible by combining the optimization criteria from Eq. 15 to Eq. 18. The performance of a selection of these hybrid scenarios are summarized in Table 6.

Regarding the price-based scenarios, the addition of minimizing total energy use could counteract the overshoot with respect to the price profile. For the Price G scenario, the addition of minimizing energy use in the optimization criterion (Energy+Price G) slightly improves the attained savings from 32% to 38%. However, for the Price I scenario, adding the minimization of energy use in the optimization criterion (Energy+Price I) drastically decreases the attained savings from 72% to 41%.

Table 5: Metrics of the residual load curve ($d_j^{trad} + nb \cdot d_j^{HP} - cur_j \cdot g_j^{RES}$), similar to Corbin [47], for the case of a 30% RES share and 250,000 buildings with heat pumps.

Name	Reference	Best case	Price G	Price I	Load Shaping
Heat pump electricity use (TWh)	1.99	2.41	2.39	2.27	2.32
Peak (GW)	12.6	11.9	12.8	12.3	12.0
Mean ramping (MW/h)	452	367	502	429	378

In this combined case, the price profile triggers the correct behavior far less.

In practice, the Load Shaping scenario may be difficult to implement as compensating the participating building owners is not straightforward. By combining this scenario with a fluctuating price profile, this compensation could be easier. The combination of the price from the integrated model with the load shaping (Price I+Load) attains a slightly higher percentage of the operational cost savings (90%) than the load shaping scenario (85%). However, this cost function proved to be difficult to handle for the buildings, as in some days it drives the temperature close to its bounds in order to attain more drastic electricity demand profiles. These issues were not observed in the combination of the three scenarios (Energy+Price I+Load). This final hybrid scenario performs very well in terms of operational cost savings and attains 93% of the maximal possible operational cost savings.

4. Discussion

Load shifting applied to building portfolios with electrically driven heat pumps provides value for the electricity generation system, as it can contribute to lowering system operational costs and CO_2 emissions (Table 3). For a low number of buildings or a low RES share, these savings are about 1% and hence rather limited. As the number of buildings or RES share increases, the reductions in operational cost and CO_2 emissions go up to 5% and 6.5% respectively. This is not a drastic change, but is nonetheless a significant contribution. For these cases, the cost savings are typically around 100 EUR per participant per year. Given the typical investment cost of enabling technologies such as the smart thermostat [8] or smart controllers [14] between 200 EUR and 350 EUR, the pay-back period is on the order of magnitude of a few years, for the boundary conditions employed in this study and assuming that all cost savings are directly attributed to the building owners. The order of magnitude of the annual reduction in CO_2 emissions is around 1 ton per participant but highly depends on the number of participating buildings and the RES share.

Regarding the magnitude of the operational cost savings of load shifting, Hedegaard and Münster [48] investigated the value of flexible operation of heat pumps in 716,000 buildings for an electricity generation system with a 60% share of wind generation and biomass fired combined heat and power plants. According to Hedegaard and Münster [48], this flexible operation results in an annual cost saving per participant of 30 EUR due to avoided operational costs and a 2% reduction in CO_2 emissions. When comparing these results with Table 3, the savings are on the same order of magnitude, but are not close. Given the similar climate, building and heat pump characteristics in both studies, the differences in savings are dominated by the composition of the electricity generation system. This difference, along with the large spread of results in Table 3, illustrates that the reductions in operational cost and CO_2 emissions are highly case dependent.

Figure 4c illustrates the avalanche effect as discussed by Dallinger and Wietschel [45] for the Price G scenario: all heat pump controllers simultaneously observe a low electricity price and drastically increase demand in those moments. Kelly et al. [18] also observed this overconsumption due to low prices, along with a loss of load diversity. As shown by Ling and Chassin [19], this loss of load diversity can cause simultaneous oscillations in electricity demand of thermostatically controlled loads, causing problems for the electricity generation system following the low price period. As proposed by Dallinger and Wietschel [45], when all participants make individual price forecasts, the peak electricity demand is less concentrated and also the load diversity is better preserved.

The Load Shaping scenario suffers far less from the above mentioned effects. First, during the moments of curtailment, the buildings do not receive a low electricity price but information to increase demand and, equally important, up to which level to increase demand. In the hour 27 in Figure 4a for example, there is little curtailment of RES and the buildings know that only a limited increase of electricity demand is necessary. This is far more information than a price signal can hold. Second, the optimization criterion of the Load Shaping scenario, Eq. 18, shows that the centrally-suggested demand curve (d_j^{IM}) is merely a suggestion, not an obligation, towards increasing or decreasing electricity demand. Part of the optimization criterion is still the electricity use minimization of each individual building. This partly ensures the preservation of load diversity, as each building will make an individual trade-off. Nonetheless, preservation of load diversity could be improved even more by providing each building with a certain perturbation on the centrally-suggested demand curve [45].

The results for the different scenarios (Figure 5) show the potential benefit of applying the integrated optimization during the day ahead stage and distributing profiles from this source. The resulting price profile (Price I scenario) clearly outperforms the case where the price profile is unilaterally determined from the electricity generation system (Price G scenario). The Price I scenario can be regarded as the case where the electricity price is infinitely iterated between electricity generation system and the individual buildings. As Figure 5b shows, this price profile causes the system to attain a great amount of the theoretically possible savings, as long as the number of participating buildings remains small. In this sense the buildings are *price takers* up to this point, and will only have a minor effect on the price itself. As the number of participating buildings increases, this influence will no longer be negligible and the buildings become *price influencers*. In this sense, the approach of suggesting a load profile instead of a price profile (the Load Shaping scenario) is generally better for a high number of participating buildings, over $100,000$ in this study. The relative operational cost savings remain stable in this scenario, even for $500,000$ participating buildings. On a total of 4.6 million households in Belgium [49], this is still a relatively small amount of participating buildings.

From the presented results, one should carefully consider whether time-of-use pricing is the correct way to achieve load shifting. In regions where a high share of the buildings employ electricity for either heating or cooling, a price profile can lead to unintended adverse effects. With the increasing share of smart thermostats [8], which are technically able to act upon such price profiles, these artifacts of greedy control actions could occur shortly afterwards. In these regions, a central determination of a load profile for all buildings to follow, appears to be a better option.

The paper only investigates the effects of different load shifting incentives for low-energy buildings. Patteeuw et al. [23] showed that buildings lacking proper insulation are not suitable candidates for heat pumps, at least not in a Belgian context. Hence, these buildings were not included in this paper.

With respect to compensation for the building owner, either a yearly fee or a tempered price profile is possible. A yearly compensation can be based on the operational cost savings as presented in Table 3, although it can be a challenge to determine which party is responsible for paying this compensation. A tempered price profile can be used in a hybrid scenario, such as in the Energy+Price I+Load scenario, to automatically compensate the building owners.

For implementing the Load Shaping scenario in practice, the procedure can be followed as shown in Figure 3. A day ahead integrated optimization of the electricity generation system along with an aggregated representation of the building stock could be performed. The resulting load profile is communicated to the generation system operators to determine their dispatch. Furthermore, the centrally-suggested demand curve (d_j^{IM}) is communicated to the smart thermostats of all participating buildings, with a small perturbation applied in order to maintain load diversity. The electricity generation system thus runs business as usual, albeit in providing an altered electricity demand profile.

5. Conclusion

In this paper, results are presented of modeling two perspectives on load shifting for heat pumps. The first perspective is the classical operational cost minimization of the electricity generation system by means of a unit commitment and economic dispatch model. The second perspective is that of a set of building owners which each possess a model predictive controller for their heating system. By modeling the two perspectives, an assessment is possible of reductions in both operational costs and CO_2 emissions due to load shifting. Additionally, an integrated formulation of the two perspectives is employed in order to determine the upper bound of operational cost and CO_2 emission reductions. Note that perfect predictions and absence of model mismatch are assumed in this study.

In the studied cases, this integrated formulation shows reductions in operational costs between 0.9% and 5.5%, depending on the number of participating buildings and the share of RES in the electricity generation. In addition, a reduction of CO_2 emissions is observed to be between 0.4% and 6.6%. These savings result from a better part-load operation of the power plants, a reduction in starting up and ramping of power plants and the reduction in curtailment of electricity generation from RES.

Multiple scenarios for a more practical load shifting application are studied, inspired by time-of-use pricing and direct-load control. The added value of the integrated formulation is shown, as it produces price profiles that clearly outperform price profiles coming from the electricity generation system optimization alone. However, as soon as a large amount of buildings, identified to be $100,000$ in this study, start participating in load shifting, the performance of price profiles drops significantly.

In general, and surely for a large amount of participants, it is shown that Load Shaping clearly outperforms the price-based incentives. Load Shaping gives clear information on the magnitude of RES curtailment and inefficient part-load operation of electricity generation plants. For this scheme, it does not matter how many buildings are participating, the performance remains in the same order of magnitude.

Finally, the authors suggest that a practical implementation of this load shifting approach may be performed centrally, namely by performing the day-ahead optimization of the operation of the electricity generation system and an aggregated formulation of the building portfolio with heat pumps. The resulting load profile can then be communicated to the buildings as a suggestion on how to shape the heat pump electricity demand over time.

6. Acknowledgement

Dieter Patteeuw, gratefully acknowledges the KU Leuven for funding this work in the framework of his PhD within the GOA project 'Fundamental study of a greenhouse gas emission-free energy system'. The authors would like to thank Kenneth Bruninx, Kenneth Van Den Bergh and Erik Delarue for providing data and advice on the Belgian electricity generation system. The authors also thank Kenneth Bruninx and Anthony R. Florita for careful review of the manuscript. The computational resources and services used in this work were provided by the Hercules Foundation and the Flemish Government- department EWI.

Appendix A. Integrated model

The integrated model combines the electricity generation system model with an optimal control formulation of the buildings with heat pumps. First, the equations of the electricity generation system model are given, which are based on Van den Bergh et al. [26]. The optimization criterion is to minimize total operational cost over all timesteps with index j:

$$min \quad \sum_i \sum_j fc_{i,j} + co_2t_{i,j} + sc_{i,j} + rc_{i,j}. \tag{A.1}$$

For each power plant with index i, the generation level ($g_{i,j}^{PP}$) and commitment status (binary variable $z_{i,j}$) determine the fuel cost ($fc_{i,j}$), CO_2 cost ($co_2t_{i,j}$), start-up cost ($sc_{i,j}$) and ramping cost ($rc_{i,j}$):

$$\forall i, \forall j : fc_{i,j} = c_i \cdot z_{i,j} + ma_i \cdot (g_{i,j}^{PP} - g_i^{min} \cdot z_{i,j}) \tag{A.2}$$

$$\begin{aligned}\forall i, \forall j : co_2t_{i,j} = co_2p \cdot [&b_i \cdot z_{i,j} \\ &+ mb_i \cdot (g_{i,j}^{PP} - g_i^{min} \cdot z_{i,j})]\end{aligned} \tag{A.3}$$

$$\forall i, \forall j : sc_{i,j} = stco_i \cdot v_{i,j} \tag{A.4}$$

$$\forall i, \forall j : rc_{i,j} \geq raco_i \cdot (g_{i,j}^{PP} - g_{i,j-1}^{PP} - v_{i,j} \cdot g_i^{max}) \tag{A.5}$$

$$\forall i, \forall j : rc_{i,j} \geq raco_i \cdot (g_{i,j-1}^{PP} - g_{i,j}^{PP} - w_{i,j} \cdot g_i^{max}) \tag{A.6}$$

in which the binary variables $v_{i,j}$ and $w_{i,j}$ respectively denote a start-up or shut-down of power plant i in time step j. The parameter c_i is the fuel cost for running the plant at its minimum power level (g_i^{min}) and ma_i is the marginal cost for the generation level on top of the minimum power level. The CO_2 emissions also consist of an emission b_i at minimum power level and a term accounting for the marginal emissions (mb_i). The CO_2 cost is then determined via a CO_2 price co_2p. Furthermore, $stco_i$ and $raco_i$ respectively denote the start-up cost and ramping cost of power plant i. The power plants are submitted to a series of technical constraints, different per fuel and technology:

$$\forall i, \forall j : g_{i,j}^{PP} \leq g_i^{max} \cdot z_{i,j} \tag{A.7}$$

$$\forall i, \forall j : g_{i,j}^{PP} \geq g_i^{min} \cdot z_{i,j} \tag{A.8}$$

$$\forall i, \forall j : g_{i,j}^{PP} \leq g_{i,j-1}^{PP} + \Delta_i^{max,up} \tag{A.9}$$

$$\forall i, \forall j : g_{i,j}^{PP} \geq g_{i,j-1}^{PP} - \Delta_i^{max,down} \tag{A.10}$$

$$\forall i, \forall j : 1 - z_{i,j} \geq \sum_{j'=j+1-mdt_i}^{j} w_{i,j'} \tag{A.11}$$

$$\forall i, \forall j : z_{i,j} \geq \sum_{j'=j+1-mut_i}^{j} v_{i,j'} \tag{A.12}$$

$$\forall i, \forall j : z_{i,j-1} - z_{i,j} + v_{i,j} - w_{i,j} = 0 \tag{A.13}$$

with g_i^{max} the maximum power level. The maximum ramping-up ($\Delta_i^{max,up}$) and maximum ramping-down ($\Delta_i^{max,down}$) values are derived from the maximum ramping rates of the power plants. The minimum up-time and down-time of power plant i are denoted by mut_i and mdt_i respectively.

The market clearing condition couples the electricity generation system model and the optimal control formulation of the buildings with heat pumps:

$$\forall j : d_j^{trad} + nb \cdot d_j^{HP} = cur_j \cdot g_j^{RES} + \sum_i g_{i,j}^{PP} \tag{A.14}$$

$$\forall j : \quad 0 \leq cur_j \leq 1 \tag{A.15}$$

with cur_j determining the amount of curtailment of the electricity generation (g_j^{RES}). The demand consists of the traditional electricity demand (d_j^{trad}) to which the scaled up (with factor nb) demand of the heat pumps (d_j^{HP}) is added. The following equations denote the optimal control formulations of the buildings with heat pumps, as described by Patteeuw and Helsen [34]. The demand d_j^{HP} is a sum of the electricity demand of multiple buildings with index s:

$$\sum_j d_j^{HP} = \sum_s \left(p_{s,j}^{HP} + p_{s,j}^{AUX}\right) \tag{A.16}$$

$$\tag{A.17}$$

and consists of the positive electricity demand of the heat pump $p_{s,j}^{HP}$ and an auxiliary electrical resistance heater $p_{s,j}^{AUX}$. These positive demands are split up over delivering space heating (suffix sh) and DHW (suffix dhw) and are limited as follows

$$\forall j : p_{s,j}^{HP,sh} + p_{s,j}^{HP,dhw} \leq p^{HP,max} \tag{A.18}$$

$$\forall j : p_{s,j}^{AUX,sh} + p_{s,j}^{AUX,dhw} \leq p^{AUX,max} \tag{A.19}$$

with $p^{HP,max}$ the maximum electric power of the heat pump which is predetermined and fixed each optimization horizon. The heat pumps are assumed to modulate perfectly. The maximum power of the auxiliary heater ($p^{AUX,max}$) is always the same value. As opposed to Eq. (6), the state space model for building and DHW tank are split up in this appendix. The state space model of the building, with temperature states $t_{s,j+1}^{sh}$ and state space matrices $\mathbf{A}^{sh}$ and $\mathbf{B}^{sh}$, is as follows

$$\begin{aligned}\forall s, j : t_{s,j+1}^{sh} &= \mathbf{A}^{sh} \cdot t_{s,j}^{sh} \\ &+ \mathbf{B}^{sh} \cdot [p_{s,j}^{HP,sh}, p_{s,j}^{AUX,sh}, t_j^E, t_j^G, q_j^S, q_{s,j}^I]\end{aligned} \tag{A.20}$$

and is submitted to the disturbances of ambient temperature (t_j^E), solar heat gain q_j^S and internal heat gains $q_{s,j}^I$. Some of the temperature states are constrained by minimum ($t_{s,j}^{sh,min}$) and maximum ($t_{s,j}^{sh,max}$) temperatures in order to maintain thermal comfort

$$\forall s, j : t_{s,j}^{sh,min} \leq t_{s,j} \leq t_{s,j}^{sh,max}. \tag{A.21}$$

The DHW tank is assumed to be a perfectly mixed storage tank. This tank could be heated up above the maximum temperature that the heat pump can attain (t_{max}^{hp}) by the auxiliary heater. In order to avoid the need for an integer variable, Patteeuw and Helsen [34] formulated a linear alternative. This defines the tank temperature $t_{s,j}^{tank}$ as the sum of a temperature which is influenced by the heat pump $t_{s,j}^{hp}$ and a temperature difference influenced by the auxiliary heater $dt_{s,j}^{aux}$ (the latter for the temperature range above t_{max}^{hp}, typically $60\,°C$). The model equations are:

$$\begin{aligned}\forall s, j : \rho c_p v_s^{tank} \frac{1}{\Delta t}(t_{s,j+1}^{hp} - t_{s,j}^{hp}) &= p_{s,j}^{aux1,dhw} \\ + cop^{dhw} \cdot p_{s,j}^{HP,dhw} - \dot{q}_{s,j}^{hp,dem} &- ua_s \cdot (t_{s,j}^{hp} - t^{surr})\end{aligned} \tag{A.22}$$

$$\begin{aligned}\forall s, j : \rho c_p v_s^{tank} \frac{1}{\Delta t}(dt_{s,j+1}^{aux} - dt_{s,j}^{aux}) &= p_{s,j}^{aux2,dhw} \\ - \dot{q}_{s,j}^{aux,dem} - ua_s \cdot (dt_{s,j}^{aux})&\end{aligned} \tag{A.23}$$

with ρ and c_p respectively the density and heat capacity of water. The time step is denoted as Δt. The COP for delivering DHW (cop^{dhw}) is predetermined and assumed constant throughout the optimization horizon. The DHW tank in each building with index s has a certain volume v_s^{tank} and thermal conductance ua_s^{tank}. Further constraints are

$$\forall s, j : \dot{q}_{s,j}^{hp,dem} + \dot{q}_{s,j}^{aux,dem} = \dot{q}_{s,j}^{dem} \tag{A.24}$$

$$\forall s, j : p_{s,j}^{aux1,dhw} + p_{s,j}^{aux2,dhw} = p_{s,j}^{AUX,dhw} \tag{A.25}$$

$$\forall s, j : t_{s,j}^{hp} \leq t_{max}^{hp} \tag{A.26}$$

$$\forall s, j : t_{s,j}^{hp} \geq t^{dem} \cdot hwd_j + t^{cold} \cdot (1 - hdw_{s,j}) \tag{A.27}$$

$$\forall s, j : (t_{max}^{tank} - t_{max}^{hp}) \geq dt_{s,j}^{aux} \geq 0. \tag{A.28}$$

The heat demand $\dot{q}_j^{dem}$ for supplying DHW has to be extracted either from the tank temperature influenced by the heat pump ($\dot{q}_j^{hp,dem}$) or from the temperature difference influenced by the auxiliary heater ($\dot{q}_j^{aux,dem}$). The heat pump can hence only heat up $t_{s,j}^{hp}$ to t_{max}^{hp}. The auxiliary heater can supply heat to both the tank temperature influenced by the heat pump ($p_{s,j}^{aux1,dhw}$) and the temperature difference influenced by the auxiliary heater ($p_{s,j}^{aux2,dhw}$). Finally, t_{max}^{tank} denotes the maximum allowable DHW tank temperature, t^{cold} the temperature of cold tap water and t^{dem} the minimum tank temperature needed when occupants demand hot water (denoted by the boolean $hdw_{s,j}$).

Appendix B. References

[1] X. He, L. Hancher, I. Azevedo, N. Keyaerts, L. Meeus, J.-M. Glachant, Shift, not drift: towards active demand response and beyond, Tech. rep., THINK project (2013).
URL `http://www.eui.eu/Projects/THINK/Documents/Thinktopic/Topic11digital.pdf`

[2] G. Strbac, Demand side management: Benefits and challenges, Energy policy 36 (12) (2008) 4419–4426.

[3] C. Gellings, The concept of demand-side management for electric utilities, Proceedings of the IEEE 73 (10) (1985) 1468–1470.
URL `http://ieeexplore.ieee.org/xpls/abs_all.jsp?arnumber=1457586`

[4] P. Palensky, D. Dietrich, Demand side management: Demand response, intelligent energy systems, and smart loads, Industrial Informatics, IEEE Transactions on 7 (3) (2011) 381–388.

[5] J. Wang, M. Biviji, W. M. Wang, et al., Lessons learned from smart grid enabled pricing programs, in: Power and Energy Conference at Illinois (PECI), IEEE, 2011, pp. 1–7.

[6] B. Dupont, Residential demand response based on dynamic electricity pricing: Theory and practice, Ph.D. thesis, KU Leuven, Belgium (2015).

[7] M. H. Albadi, E. El-Saadany, A summary of demand response in electricity markets, Electric power systems research 78 (11) (2008) 1989–1996.

[8] Grand View Research, Smart thermostat market analysis by technology (Wi-Fi, ZigBee) and segment forecasts to 2022, Tech. rep. (September 2015).
URL `http://www.grandviewresearch.com/industry-analysis/smart-thermostat-market`

[9] J. Lu, T. Sookoor, V. Srinivasan, G. Gao, B. Holben, J. Stankovic, E. Field, K. Whitehouse, The smart thermostat: using occupancy sensors to save energy in homes, in: Proceedings of the 8th ACM Conference on Embedded Networked Sensor Systems, ACM, 2010, pp. 211–224.

[10] Y. Matsuoka, Our first rush hour rewards results., Online (July 2013).
URL `https://nest.com/blog/2013/07/18/our-first-rush-hour-rewards-results/`

[11] D. S. Callaway, Tapping the energy storage potential in electric loads to deliver load following and regulation, with application to wind energy, Energy Conversion and Management 50 (5) (2009) 1389–1400.

[12] J. Mathieu, M. Dyson, D. Callaway, A. Rosenfeld, Using residential electric loads for fast demand response: The potential resource and revenues, the costs, and policy recommendations, in: Proceedings of the ACEEE Summer Study on Buildings, Pacific Grove, CA, 2012, pp. 189–203.

[13] D. Wang, S. Parkinson, W. Miao, H. Jia, C. Crawford, N. Djilali, Online voltage security assessment considering comfort-constrained demand response control of distributed heat pump systems, Applied Energy 96 (2012) 104–114.

[14] K. Hedegaard, B. V. Mathiesen, H. Lund, P. Heiselberg, Wind power integration using individual heat pumps - analysis of different heat storage options, Energy 47 (1) (2012) 284–293.

[15] J. Barton, S. Huang, D. Infield, M. Leach,

D. Ogunkunle, J. Torriti, M. Thomson, The evolution of electricity demand and the role for demand side participation, in buildings and transport, Energy Policy 52 (2013) 85–102.

[16] M. Kamgarpour, C. Ellen, S. Esmaeil, Z. Soudjani, S. Gerwinn, J. L. Mathieu, M. Nils, A. Abate, D. S. Callaway, M. Fr, Modeling Options for Demand Side Participation of Thermostatically Controlled Loads, in: IREP Symposium-Bulk Power System Dynamics and Control -IX (IREP), August 25-30, 2013, Rethymnon, Greece, 2013, pp. 1–15.

[17] G. P. Henze, C. Felsmann, G. Knabe, Evaluation of optimal control for active and passive building thermal storage, International Journal of Thermal Sciences 43 (2) (2004) 173–183.

[18] N. J. Kelly, P. G. Tuohy, A. D. Hawkes, Performance assessment of tariff-based air source heat pump load shifting in a UK detached dwelling featuring phase change-enhanced buffering, Applied Thermal Engineering.
URL `http://dx.doi.org/10.1016/j.applthermaleng.2013.12.019`

[19] N. Lu, D. P. Chassin, A state-queueing model of thermostatically controlled appliances, Power Systems, IEEE Transactions on 19 (3) (2004) 1666–1673.

[20] F. Oldewurtel, A. Ulbig, A. Parisio, G. Andersson, M. Morari, Reducing peak electricity demand in building climate control using real-time pricing and model predictive control, in: Decision and Control (CDC), 49th IEEE Conference on, pp. 1927–1932.

[21] B. Dupont, C. De Jonghe, L. Olmos, R. Belmans, Demand response with locational dynamic pricing to support the integration of renewables, Energy Policy 67 (2014) 344–354.

[22] B. Dupont, K. Dietrich, C. De Jonghe, A. Ramos, R. Belmans, Impact of residential demand response on power system operation: A Belgian case study, Applied Energy 122 (2014) 1–10.

[23] D. Patteeuw, G. Reynders, K. Bruninx, C. Protopapadaki, E. Delarue, W. D'haeseleer, D. Saelens, L. Helsen, CO_2 -abatement cost of residential heat pumps with active demand response: demand- and supply-side effects, Applied Energy 156 (2015) 490 – 501.

[24] J. Širokỳ, F. Oldewurtel, J. Cigler, S. Prívara, Experimental analysis of model predictive control for an energy efficient building heating system, Applied Energy 88 (9) (2011) 3079–3087.

[25] M. C. Ferris, R. Jain, S. Dirkse, GDXMRW : Interfacing GAMS and MATLAB (2011).
URL `http://www.gams.com/dd/docs/tools/gdxmrw.pdf`

[26] K. Van den Bergh, K. Bruninx, E. Delarue, W. D'haeseleer, LYSUM: a mixed-integer linear formulation of the unit commitment problem, KU Leuven Energy Institute Working papers EN2014-07 (2014) 1–20.
URL `http://www.mech.kuleuven.be/en/tme/research/energy_environment/Pdf/wpen2014-07.pdf`

[27] D. Patteeuw, K. Bruninx, E. Delarue, L. Helsen, W. D'haeseleer, Short-term demand response of flexible electric heating systems : an integrated model, KU Leuven Energy Institute Working Paper WP2014-28 (2014).
URL `http://www.mech.kuleuven.be/en/tme/research/energy_environment/Pdf/wpen2014-28.pdf`

[28] ENTSO-E, Internal document (2013).

[29] K. Bruninx, E. Delarue, W. Dhaeseleer, The cost of wind power forecast errors in the belgian power system, in: 2nd BAEE Research Workshop,(Leuven, Belgium), 2013, pp. 1–20.

[30] ELIA, Grid data (2013).
URL `http://www.elia.be/nl/grid-data`

[31] A. Schröder, F. Kunz, J. Meiss, R. Mendelevitch, C. Von Hirschhausen, Current and prospective costs of electricity generation until 2050, DIW Data Documentation 68.

[32] D. Devogelaer, J. Duerinck, D. Gusbin, Y. Marenne, W. Nijs, M. Orsini, M. Pairon, Towards 100% renewable energy in Belgium by 2050, VITO, Mol (2013, April).

[33] G. Reynders, J. Diriken, D. Saelens, Bottom-up modelling of the Belgian residential building stock: influence of model complexity, in: International Conference on System Simulation in Buildings Edition 9, Liège, Belgium, 2014, pp. 574–592.

[34] D. Patteeuw, L. Helsen, Residential buildings with heat pumps, a verified bottom-up model for demand side management studies, in: International Conference on System Simulation in Buildings Edition 9, Liège, Belgium, 2014, pp. 498–516.

[35] C. Protopapadaki, G. Reynders, D. Saelens, Bottom-up modelling of the Belgian residential building stock: impact of building stock descriptions, in: International Conference on System Simulation in Buildings Edition 9, Liège, Belgium, 2014, pp. 652–672.

[36] R. Baetens, D. Saelens, Modelling uncertainty in district energy simulations by stochastic residential occupant behaviour, Journal of Building Performance Simulation (2015) 1–17`doi:10.1080/19401493.2015.1070203`.

[37] I. Richardson, M. Thomson, D. Infield, A high-resolution domestic building occupancy model for energy demand simulations, Energy and buildings 40 (8) (2008) 1560–1566.

[38] W. Cyx, N. Renders, M. Van Holm, S. Verbeke, IEE TABULA typology approach for build-

ing stock energy assessment, Tech. rep., VITO, Vlaamse instelling voor technologisch onderzoek (2011).

[39] G. Verbeeck, Optimisation of extremely low energy residential buildings, phd-thesis, K.U.Leuven, Belgium (2007).

[40] K. Bettgenhäuser, M. Offermann, T. Boermans, M. Bosquet, J. Grözinger, B. von Manteuffel, N. Surmeli, Heat pump implementation scenarios until 2030, appendix, Tech. rep., Ecofys (2013).

[41] C. Verhelst, F. Logist, J. Van Impe, L. Helsen, Study of the optimal control problem formulation for modulating air-to-water heat pumps connected to a residential floor heating system, Energy and Buildings 45 (2012) 43–53.

[42] D. Patteeuw, K. Bruninx, A. Arteconi, E. Delarue, W. Dhaeseleer, L. Helsen, Integrated modeling of active demand response with electric heating systems coupled to thermal energy storage systems, Applied Energy 151 (2015) 306–319.

[43] C. D. Corbin, G. P. Henze, Residential HVAC as a supply following resource part i: Simulation framework and model development, IEEE Transactions on Power Systems.

[44] C. D. Corbin, G. P. Henze, Residential HVAC as a supply following resource part ii: Simulation studies and results, IEEE Transactions on Power Systems.

[45] D. Dallinger, M. Wietschel, Grid integration of intermittent renewable energy sources using price-responsive plug-in electric vehicles, Renewable and Sustainable Energy Reviews 16 (5) (2012) 3370–3382.

[46] A. Arteconi, D. Patteeuw, K. Bruninx, E. Delarue, W. Dhaeseleer, L. Helsen, Active demand response with electric heating systems: impact of market penetration, Submitted to Energy (2015) 1–19.

[47] C. D. Corbin, Assessing impact of large-scale distributed residential HVAC control optimization on electricity grid operation and renewable energy integration, Ph.D. thesis, University of Colorado, CO, U.S.A. (2014).

[48] K. Hedegaard, M. Münster, Influence of individual heat pumps on wind power integration–energy system investments and operation, Energy Conversion and Management 75 (2013) 673–684.

[49] FPS Economy Belgium, Structure of the population according to households: per year, region and number of children, Online: `http://statbel.fgov.be/nl/statistieken/cijfers/bevolking/structuur/huishoudens/`.